PHYSICAL REVIEW B **80**, 241109(R) (2009)

Anomalous nonergodic scaling in adiabatic multicritical quantum quenches

Shusa Deng,[1] Gerardo Ortiz,[2] and Lorenza Viola[1]
[1]*Department of Physics and Astronomy, Dartmouth College, 6127 Wilder Laboratory, Hanover, New Hampshire 03755, USA*
[2]*Department of Physics, Indiana University, Bloomington, Indiana 47405, USA*
(Received 31 August 2009; published 30 December 2009)

We investigate nonequilibrium dynamical scaling in adiabatic quench processes across quantum multicritical points. Our analysis shows that the resulting power-law scaling *depends sensitively on the control path* and that anomalous critical exponents may emerge depending on the universality class. We argue that the observed anomalous behavior originates in the fact that the dynamical excitation process takes place asymmetrically with respect to the static multicritical point and that noncritical energy modes may play a dominant role. As a consequence, dynamical scaling requires introducing genuinely nonstatic exponents.

DOI: 10.1103/PhysRevB.80.241109 PACS number(s): 73.43.Nq, 75.10.Jm, 64.60.Kw, 05.30.−d

I. INTRODUCTION

Establishing dynamical scaling relations in many-body systems adiabatically driven out-of-equilibrium across a quantum phase transition has important implications for both condensed-matter physics[1] and adiabatic quantum computation.[2] A paradigmatic scenario is the Kibble-Zurek scaling (KZS),[3,4] whereby a homogeneous d-dimensional system is linearly driven with a constant speed $1/\tau$ across an isolated quantum critical point (QCP) described by equilibrium critical exponents ν and z. Assuming that in the thermodynamic limit, the system loses adiabaticity throughout an "impulse region" $[t_c-\hat{t},t_c+\hat{t}]$ centered around the QCP and with a characteristic width $2\hat{t}$, excitations are generated in the final state with a density $n_{\mathrm{ex}}(t_f)\sim\tau^{-d\nu/(\nu z+1)}$. While the KZS and its nonlinear generalizations have been verified in several exactly solvable models,[5] departures from the KZ prediction may occur for more complex quench processes, involving isolated QCPs in disordered[6] and infinitely coordinated systems[7] or nonisolated QCPs (that is, quantum critical regions).[8–10] Evidence of non-KZS, however, has also been reported in the apparently simpler situation of a quench across a single quantum multicritical point (MCP) in clean spin chains.[11,12]

In this work, we show how multicritical quantum quenches dramatically exemplify the dependence of nonequilibrium scaling upon the control path anticipated in Ref. 9 and demonstrate that anomalous "nonergodic" scaling may emerge in the thermodynamic limit. While a non-KZS $n_{\mathrm{ex}}(t_f)\sim\tau^{-1/6}$ was previously reported[11] and an explanation given in terms of an "effective dynamical critical exponent" $z_2=3$, the meaning of such exponent relied on the applicability of a Landau-Zener (LZ) treatment, preventing general insight to be gained. We argue that the failure of KZS is physically rooted in the shift of the center of the impulse region relative to the static picture and that z_2 is determined by the scaling of a path-dependent *minimum gap*, which need not coincide with the critical gap. Furthermore, such a dynamical shift may also cause the contribution from *intermediate noncritical energy states* to dominate the scaling of the excitation density, via an "effective dimensionality exponent" $d_2\neq 0$. We show that the latter leads to the emergence of a new scaling behavior $n_{\mathrm{ex}}(t_f)\sim\tau^{-3/4}$. A unified understanding is obtained by extending the adiabatic renormalization (AR) approach of Ref. 9.

II. MODEL HAMILTONIAN

We focus on the alternating spin-1/2 XY chain described by the Hamiltonian[9,13]

$$H=-\sum_{i=1}^{N}(\gamma_+\sigma_x^i\sigma_x^{i+1}+\gamma_-\sigma_y^i\sigma_y^{i+1}-h_i\sigma_z^i), \tag{1}$$

where $\gamma_\pm=(1\pm\gamma)/2$, $h_i=h-(-)^i\delta$, and periodic boundary conditions are assumed. Here, $h,\delta\in\mathbb{R}$ are the uniform and alternating magnetic field strength, respectively, whereas $\gamma\in\mathbb{R}$ is the anisotropy (lifting the restriction $\gamma\in[0,1]$ is essential for the present analysis). An exact solution for the energy spectrum of H may be obtained through the steps outlined in Ref. 13. The problem maps into a collection of noninteracting quasiparticle labeled by momentum modes $k\in K_+=\{\pi/N,3\pi/N,\ldots,\pi/2-\pi/N\}$, whose excitation gap is given by $\Delta_k(\gamma,h,\delta)=4[h^2+\delta^2+\cos^2 k+\gamma^2\sin^2 k-2\sqrt{h^2\cos^2 k+\delta^2(h^2+\gamma^2\sin^2 k)}]^{1/2}$. The quantum phase boundaries are determined by the equations[9,13] $h^2=\delta^2+1$, $\delta^2=h^2+\gamma^2$. Thus, the critical lines on the $\gamma=0$ plane consist entirely of MCPs.

III. QUENCH DYNAMICS: EXACT RESULTS

We assume that the system is initially in the ground state and that (in the simplest case) a slow quench across a MCP is implemented upon changing a single control parameter according to $\delta\lambda(t)=\lambda(t)-\lambda_c=|(t-t_c)/\tau|^\alpha\mathrm{sign}(t-t_c)$ over a time interval $t\in[t_0,t_f]$, where $\alpha=1$ corresponds to a linear driving, and λ_c is the critical value. Thus, the time-dependent Hamiltonian $H(t)$ may be written as $H(t)=H_c+\delta\lambda(t)H_1$, where H_c is quantum multicritical at time t_c in the thermodynamic limit, and H_1 is the contribution that couples to the external control (a similar parametrization is possible for quenches involving multiple parameters). Without loss of generality, we may let $t_c=0$. In what follows, we shall focus on two representative MCPs, A and B as marked in Fig. 1, each approached through two different paths (path 5 will be

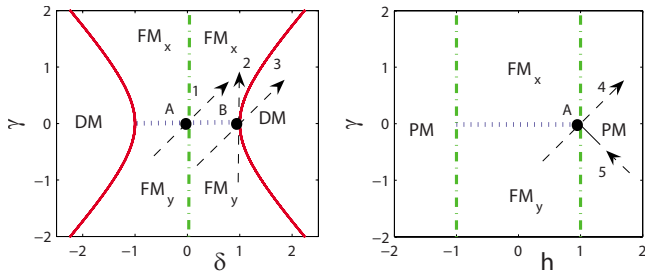

FIG. 1. (Color online) Phase diagram of H in Eq. (1) when $h=1$ (left) and $\delta=0$ (right). The dashed-dotted (green) line separates the ferromagnetic (FM) and paramagnetic (PM) phases, the solid (red) lines separate dimer (DM) and FM, whereas the dotted (blue) line is the superfluid phase (SF). The arrows indicate the relevant control paths for A and B.

introduced later), whose properties are summarized in Table I.

In order to quantify the amount of excitation at a generic instant t, we numerically integrate the time-dependent Schrödinger equation for $H(t)$ and monitor two standard "nonadiabaticity" indicators:[7,9,13] the excitation density $n_{\rm ex}$ and the residual energy ΔH. For a linear quench along either path 1 or 2 (left panel of Fig. 2), we find that $n_{\rm ex}(t) \sim \tau^{-\nu/(\nu z+1)}=\tau^{-1/3}$ and $\Delta H(t)\sim\tau^{-\nu(1+z)/(\nu z+1)}=\tau^{-1}$, which is consistent with KZS[3] and our conclusion in Ref. 9. For paths 3 and 4, however (right panel of Fig. 2), we find that $n_{\rm ex}(t) \sim \tau^{-1/6}$ and $\Delta H(t)\sim\tau^{-2/3}$, which is non-KZS (in Ref. 11, the $\tau^{-1/6}$ scaling was pointed out for an equivalent quench scheme across MCP A). Similar anomalous exponents are found for nonlinear quenches along path 3 or 4, e.g., $n_{\rm ex}(t) \sim \tau^{-2/9}$ for $\alpha=2$.

The above results show that for quenches across a MCP, whether KZS is obeyed depends sensitively on which control path is chosen. A closer inspection reveals the following important differences: (i) paths 1,2 start and end in essentially the same phase, correspondingly, the excitation spectrum is invariant under a transformation $\lambda\mapsto-\lambda$ of the control parameters. Paths 3,4 do not exhibit this symmetry; (ii) along paths 3,4, the MCPs A and B belong to the Lifshitz universality class ($\nu=1/2$), although all paths share $z=2$. It is then natural to ask which of these differences may play a role in determining the anomalous dynamical scaling behavior. To answer this question, we introduce another "V-shaped" path across MCP A (path 5), $h(t)=1+|\gamma(t)|=1+|t/\tau|$, which starts and ends in the PM phase but, in each of the two segments, crosses the MCP A with Lifshitz exponents. Surprisingly, the observed scaling is $n_{\rm ex}(t)\sim\tau^{-3/4}$ (left panel of Fig. 3), which

TABLE I. Critical exponents and parametrization of the relevant control paths for MCPs A and B.

Path	ν	z	Quenching scheme
1	1	2	$\gamma(t)=\delta(t)=\lvert t/\tau\rvert^{\alpha}\mathrm{sign}(t);\ h=1$
2	1	2	$\gamma(t)=\lvert t/\tau\rvert^{\alpha}\mathrm{sign}(t);\ h=1,\delta=1$
3	1/2	2	$\gamma(t)=\delta(t)-1=\lvert t/\tau\rvert^{\alpha}\mathrm{sign}(t);\ h=1$
4	1/2	2	$\gamma(t)=h(t)-1=\lvert t/\tau\rvert^{\alpha}\mathrm{sign}(t);\ \delta=0$

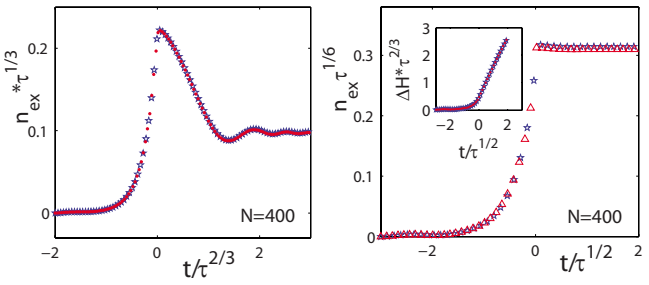

FIG. 2. (Color online) Exact scaling of the excitation density during a linear quench along path 2 (left) and path 3 (right). Right inset: scaling of the residual energy along path 3.

is neither KZS nor $-1/6$. An identical $-3/4$ scaling holds for a similar V-path across MCP B that starts and ends in the DM phase. As finite-size analysis reveals, all the observed anomalous scalings are practically independent upon system size over a wide range of quench rates (see, e.g., right panel of Fig. 3), establishing them as truly thermodynamic in nature.[14]

IV. LANDAU-ZENER ANALYSIS

We begin to seek an understanding from limiting cases, where an exact solution for $n_{\rm ex}(t_f)$ may be obtained based on the LZ picture.[15] This is possible provided that $\alpha=1$ and the Hamiltonian can be decoupled into effective two-level systems. Among the above-mentioned paths, only paths 4 and 5 (for which $\delta=0$) can be exactly mapped to a LZ problem, thanks to the possibility of rewriting H in Eq. (1) as $H=\Sigma_k\hat{H}_k=\Sigma_k B_k^\dagger H_k B_k$, where $B_k^\dagger=(c_{-k},c_k^\dagger)$ and

$$H_k=\begin{pmatrix} H_{k,11} & H_{k,12} \\ H_{k,12}^* & -H_{k,11}\end{pmatrix}=2\begin{pmatrix} -h+\cos k & \gamma\sin k \\ \gamma\sin k & h-\cos k\end{pmatrix}. \quad (2)$$

A rotation $R_k(q_k)$, $q_k\in[-\pi/2,\pi/2)$, renders the off-diagonal terms in Eq. (2) independent upon γ (hence time), allowing use of the LZ formula. Consider path 4 first. By choosing $\tan 2q_k=-\sin k$, the transformed Hamiltonian matrix elements become $H'_{k,11}=-2(1-\cos k)\cos 2q_k-2t/\tau(\cos 2q_k-\sin k\,\sin 2q_k)$, and $H'_{k,12}=2(1-\cos k)\sin 2q_k$. If the critical mode k_c is defined by requiring $\Delta_{k_c}=0$ in the thermodynamic

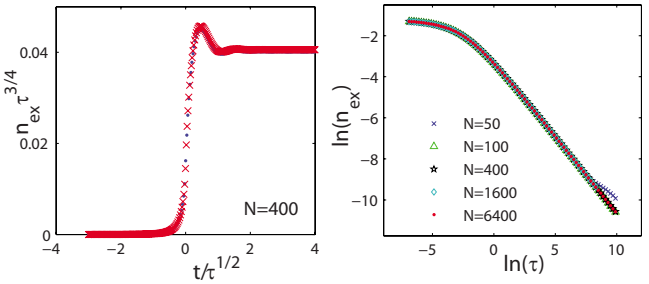

FIG. 3. (Color online) Left: exact scaling of the excitation density during a linear quench along path 5. Right: scaling of the final excitation density in path 5 for different size; $n_{\rm ex}(t_f)$ is the same to a numerical accuracy of 10^{-6}, up to $\tau<2\times10^5$. A linear fit yields -0.747 ± 0.001 over $200<\tau<2000$.

limit, we have $k_c=0$ for the MCP A. We may then let $\tan 2q_k \approx \sin 2q_k$, and the appropriate $q_k \approx -k/2$. From the LZ formula, the asymptotic ($t_f \to \infty$) excitation probability reads as

$$p_k = e^{-2\pi\tau(1-\cos k)^2 \sin^2 2q_k/(\cos 2q_k - \sin k \sin 2q_k)} \approx e^{-\pi\tau k^6/2},$$

where the approximation follows from a Taylor expansion around k_c. Integrating over all modes yields $n_{\rm ex}(t_f) \sim \tau^{-1/6}$, which is consistent with our exact numerical result. Therefore, mathematically, the $\tau^{-1/6}$ scaling follows from the fact that the exponent in p_k scales as $k^6 = k^{2z_2}$, with $z_2=3$. In turn, this originates from the scaling of the off-diagonal terms $H'_{k,12} \sim k^{z_2}$. Physically, as we shall later see by invoking AR, $H'_{k,12}$ may be interpreted as the minimum gap for mode k along path 4.

To unveil the $\tau^{-3/4}$ scaling, it is necessary to use the *exact finite-time* LZ solution. For simplicity, we restrict to half of path 5, by quenching the system from the PM phase up to the MCP A. This has the benefit of avoiding the nonanalytic time dependence of the control parameters that path 5 exhibits at A, while leaving the $\tau^{-3/4}$ scaling unchanged thanks to the symmetry of the excitation spectrum. Starting from Vitanov's expression [Eq. (7) in Ref. 16], the excitation probability $p_k(t_f)$ can be computed via the parabolic cylinder function $D_v(z)$,

$$p_k(t_f) = e^{-\pi\omega^2/4} \left| D_{i\omega^2/2}(T_f\sqrt{2}e^{i3\pi/4}) \cos\,\theta(T_f) - \frac{\omega}{\sqrt{2}} e^{-i\pi/4} D_{i\omega^2/2-1}(T_f\sqrt{2}e^{i3\pi/4}) \sin\,\theta(T_f) \right|^2,$$

where $\omega = (1-\cos k)\sin 2q_k \sqrt{\tau}/\sqrt{\cos 2q_k + \sin 2q_k \sin k} \sim k^3\sqrt{\tau}$ is the rescaled coupling strength, $T_f = -\omega/\sin k \sim -k^2\sqrt{\tau}$ is the rescaled time, $\tan 2q_k = \sin k$, and $\theta(T_f) = 1/2 \arctan(\omega/T_f) + \pi/2$. Since for our quench process $\omega \ll |T_f| \ll 1$ around k_c, we may estimate $p_k(t_f)$ by Taylor expanding $D_v(z)$ around $T_f=0$,

$$p_k(t_f) \approx (1-e^{-\pi\omega^2/2})/2 + \cos^2\,\theta(T_f) e^{-\pi\omega^2/2} - \sin 2\theta(T_f)/2 \, \sin\chi_k \sqrt{1-e^{-\pi\omega^2}}, \quad (3)$$

where $\chi_k \approx \pi/4$ around k_c. This approximation breaks when $T_f \sim 1$, setting the scaling of the highest-momentum contributing mode $k_{\rm max} \sim \tau^{-1/4}$. In Eq. (3), the dominant term $\cos^2\,\theta(T_f) e^{-\pi\omega^2/2} \sim \cos^2\,\theta(T_f) \sim |\omega/T_f|^2 \sim k^2$ since $e^{-\pi\omega^2/2} \approx 1$ within $k_{\rm max}$, which means $p_k(t_f) \sim k^2$. Thus, $n_{\rm ex}(t_f) = \int_0^{k_{\rm max}} p_k(t_f) \sim k_{\rm max}^3 \sim \tau^{-3/4}$, in agreement with our numerical results. Remarkably, the fact that $p_k(t_f) \sim (k-k_c)^{d_2}$, $d_2=2$, indicates that k_c is *not* excited despite a static QCP being crossed, and also that the *excitation is dominated by intermediate energy states*. In fact, at the MCP A, the modes around k_c are still far from the impulse region, since $|T_f| \gg \omega$, which sets the LZ transition time scale.[16] This is in stark contrast with the main assumption underlying KZS, where the center of the impulse region is the static QCP, and excitations are dominated by modes near k_c, as reflected in the typical scaling $p_k \sim (k-k_c)^0$.

Notice how the *asymmetry* of the dynamical impulse region (due to the asymmetry of the excitation spectrum) underlies the emergence of the observed anomalous scalings, in different ways: along path 4, such an asymmetry shifts the center of the impulse region into the FM phase (see also Fig. 2, right), and whether the LZ solution with $t_f \to \infty$ or $t_f \to 0^-$ is used leads to the same $\tau^{-1/6}$ result. Along half of path 5, instead, stopping the quench at MCP A is a prerequisite for "blocking" low-energy modes, and different scaling $(-1/6)$ would be obtained by extending the quench beyond $t_f=0$ into the FM phase and using the LZ asymptotic result.

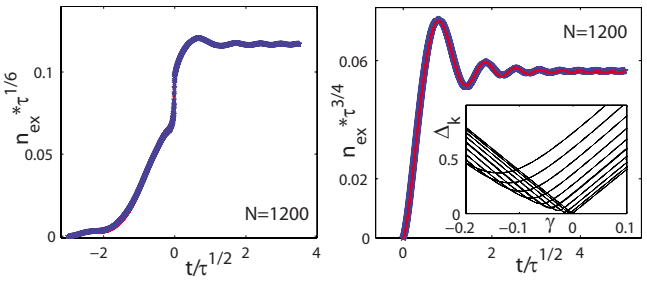

FIG. 4. (Color online) Scaling of the excitation density from first-order AR for a linear quench along path 3 (left) and half-5 starting at MCP A (right). Right inset: low-lying single-mode excitation spectrum along path 4 for $N=100$.

V. PERTURBATIVE SCALING APPROACH

Since the system becomes gapless at a single MCP along all the paths under study, first-order AR is a viable approach.[4,9] Let $|\psi_m(t)\rangle$ be a basis of snapshot eigenstates of $H(t)$, with snapshot eigenvalues $E_m(t)$, $m=0$ labeling the ground state. The time-evolved state may be expanded as $|\psi(t)\rangle = c_0^{(1)}(t)|\psi_0(t)\rangle + \Sigma_{m\neq 0} c_m^{(1)}(t)|\psi_m(t)\rangle$, where the coefficients $c_m^{(1)}(t)$ determine the excitation amplitudes and are given by Eq. (4) in Ref. 9. First-order AR calculations of $n_{\rm ex}(t)$ demonstrate that for linear quenches along paths 1 and 2, $n_{\rm ex} \sim \tau^{-1/3}$, whereas $n_{\rm ex} \sim \tau^{-1/6}$ along paths 3 and 4 (left panel of Fig. 4). Since the nonanalyticity at A in path 5 might cause problems in AR, again we choose to study half of path 5 (right panel of Fig. 4). All the AR results agree with the exact simulation results, confirming that AR reproduces the correct dynamical scaling across a *generic* isolated QCP.

Predicting the scaling exponent based on AR requires scaling assumptions for the contributions entering $c_m^{(1)}(t)$ [i.e., $\Delta_m(t) = E_m(t) - E_0(t)$ and $\langle\psi_m(t)|H_1|\psi_0(t)\rangle$], and the ability to change discrete sums of all the contributing excited states into integrals, for which the density of excited states $\rho(E)$ is required. Since typically the AR prediction is consistent with KZS, anomalous behavior must stem from anomalous scaling assumptions of (one or more of) these ingredients. We first examine the excitation spectrum along different paths. Since H_1 is a one-body perturbation, only single-mode excitations are relevant; thus, the index m labeling many-body excitations may be identified with a momentum mode. Along paths 1 and 2, it turns out that the minimum gap among all modes is *always* located at k_c, whereas along paths 3 and 4, the minimum gap is located at k_c *only* at the MCP. This suggests that knowing the static exponents of the MCP alone

need *not* suffice to determine the dynamical scaling due to the existence of "quasicritical" modes along paths 3 and 4. Mathematically, along path 4, $\partial\Delta_k(\gamma,1+\gamma,0)/\partial\gamma=0$ gives the location of the minimum gap for each mode k at $\tilde{\gamma}=(\cos k-1)/(1+\sin k^2)$, which is largely shifted into the FM phase (see inset in Fig. 4). By inserting this relation back into Δ_k, the function $\Delta_k(\tilde{\gamma})\equiv\tilde{\Delta}_k\sim(k-k_c)^3$. Following the same procedure also yields $\tilde{\Delta}_k\sim(k-k_c)^3$ along path 3, whereas $\tilde{\Delta}_k$ has the same scaling as Δ_k at the MCP along paths 1 and 2. This motivates modifying the AR scaling assumptions of Ref. 9 as follows: $E_m(t)-E_0(t)=\delta\lambda(t)^{\nu z}f_m[\Delta_m(t_{\min})/\delta\lambda(t)^{\nu z}]$, where $\Delta_m(t_{\min})$ is the minimum gap of mode m attained at $t_{\min}$ along the path, and f_m is a scaling function.

The above modification requires the scaling of $\rho(E)$ to be modified by letting $\rho(E)\sim E^{d/z_2-1}$, where z_2 comes from the dispersion relation of $\Delta_m(t_{\min})$. If the minimum gap of any mode is below a certain energy along the path, that mode should be counted into the contributing excited states. Accordingly, we have $z_2=z=2$ along paths 1, 2, half-5, and $z_2=3$ along paths 3, 4. Back to the LZ analysis, note that the off-diagonal term $H'_{12}(k)$ is the minimum gap of mode k along the path if there exists a time at which the diagonal term $H'_{11}(k)=0$, as it happens for path 4. For path 5, however, the off-diagonal term never becomes the minimum gap since the system never leaves the PM phase. Therefore, the off-diagonal term in the LZ picture need not suffice to determine the dynamical scaling, and the shift of the location of the minimum gap for each mode from the static QCP is at the root of the anomalous behavior we observe. Lastly, we consider the matrix elements of H_1. Numerical simulations suggest that $\langle\psi_m(t)|H_1|\psi_0(t)\rangle=\delta\lambda(t)^{\nu z-1}g_m[\Delta_m(t_{\min})/\delta\lambda(t)^{\nu z}]$, where g_m is a scaling function, and $\Delta_m(t_{\min})$ is the minimum gap of mode m along a path that *extends* the actual path to $t_f\to\infty$ when the quench is stopped at the MCP and coincides with the actual path otherwise. Then along paths 1 and 2, $\Delta_m(t_{\min})\sim k^2$, whereas along paths 3, 4, and half-5, $\Delta_m(t_{\min})\sim k^3$. Together with the other scaling assumptions and taking the linear case $\alpha=1$ as an example, AR yields $|c_m^{(1)}|\sim k^0$, $n_{\rm ex}\sim\tau^{-(z/z_2)(\nu/(\nu z+1))}$ along paths 1–4, and $|c_m^{(1)}|\sim k^1$, $n_{\rm ex}\sim\tau^{-3\nu/(\nu z+1)}$ along half-5 path, which completely agrees with the numerical results.

Building on the above analysis, we argue on physical grounds that the scaling of the excitation density for quenches across an *arbitrary* (*standard or multicritical*) *isolated QCP* is determined by three conditions: (i) from the condition of adiabaticity breaking, the typical gap $\hat{\Delta}$ scales as $\hat{\Delta}\sim\tau^{-\alpha\nu z/(\alpha\nu z+1)}$; (ii) an accessible excited state contributes to the excitation if and only if its minimum gap along the path matches with this typical gap $\tilde{\Delta}_k\sim\hat{\Delta}$, with $\tilde{\Delta}_k\sim(k-k_c)^{z_2}$; (iii) the excitation probability p_k scales as $p_k\sim(k-k_c)^{d_2}$, where d_2 can differ from 0 if the center of the impulse region is greatly shifted relative to the static limit. Then upon integrating up to energy $\hat{\Delta}$, and using $p_E\sim p_{k(E)}\sim E^{d_2/z_2}$, yields

$$n_{\rm ex}\sim\hat{\Delta}^{(d+d_2)/z_2}\sim\tau^{-(d+d_2)\alpha\nu z/[z_2(\alpha\nu z+1)]}, \tag{4}$$

which is consistent with all the results found thus far. While KZS corresponds to $z_2=z$, $d_2=0$, situations where $z_2\neq z$ and/or $d_2\neq 0$ are *genuinely dynamical*. The knowledge about the path-dependent excitation process becomes crucial and nonequilibrium exponents cannot be fully predicted from equilibrium ones. Interestingly, in the model under examination the Lifshitz universality class appears to be the only universality class for which anomalous scaling occurs, among all possible paths involving MCPs. Whether Lifshitz behavior may constitute a *sufficient* condition for anomalous behavior requires further investigation in other many-body systems.

ACKNOWLEDGMENTS

We thank T. Caneva for insightful feedback. S.D. acknowledges support from a Hull Graduate Foundation.

[1] S. Sachdev, *Quantum Phase Transitions* (Cambridge University Press, Cambridge, 1999).

[2] E. Farhi, J. Goldstone, S. Gutmann, J. Lapan, A. Lundgren, and D. Preda, Science **292**, 472 (2001); G. E. Santoro and E. Tosatti, J. Phys. A **39**, R393 (2006).

[3] W. H. Zurek, U. Dorner, and P. Zoller, Phys. Rev. Lett. **95**, 105701 (2005); J. Dziarmaga, *ibid.* **95**, 245701 (2005); B. Damski and W. H. Zurek, Phys. Rev. A **73**, 063405 (2006); F. M. Cucchietti, B. Damski, J. Dziarmaga, and W. H. Zurek, *ibid.* **75**, 023603 (2007).

[4] A. Polkovnikov, Phys. Rev. B **72**, 161201(R) (2005); A. Polkovnikov and V. Gritsev, Nat. Phys. **4**, 477 (2008).

[5] R. W. Cherng and L. S. Levitov, Phys. Rev. A **73**, 043614 (2006); A. Fubini, G. Falci, and A. Osterloh, New J. Phys. **9**, 134 (2007); V. Mukherjee, A. Dutta, and D. Sen, Phys. Rev. B **77**, 214427 (2008); S. Mondal, D. Sen, and K. Sengupta, *ibid.* **78**, 045101 (2008); D. Sen, K. Sengupta, and S. Mondal, Phys. Rev. Lett. **101**, 016806 (2008); R. Barankov and A. Polkovnikov, *ibid.* **101**, 076801 (2008).

[6] J. Dziarmaga, Phys. Rev. B **74**, 064416 (2006); T. Caneva, R. Fazio, and G. E. Santoro, *ibid.* **76**, 144427 (2007).

[7] T. Caneva, R. Fazio, and G. E. Santoro, Phys. Rev. B **78**, 104426 (2008).

[8] F. Pellegrini, S. Montangero, G. E. Santoro, and R. Fazio, Phys. Rev. B **77**, 140404(R) (2008).

[9] S. Deng, G. Ortiz, and L. Viola, EPL **84**, 67008 (2008).

[10] D. Chowdhury, U. Divakaran, and A. Dutta, arXiv:0906.1161 (unpublished).

[11] V. Mukherjee, U. Divakaran, A. Dutta, and D. Sen, Phys. Rev. B **76**, 174303 (2007); U. Divakaran, V. Mukherjee, A. Dutta, and D. Sen, J. Stat. Mech.: Theory Exp. 2009, P02007.

[12] S. Mondal, K. Sengupta, and D. Sen, Phys. Rev. B **79**, 045128 (2009).

[13] S. Deng, G. Ortiz, and L. Viola, *14th International Conference on Recent Progress in Many-Body Theories (RPMBT14)* (World Scientific, Singapore, 2008), Vol. 11, p. 387.

[14] Since $\nu z<z$, to leading order the scaling of Δ_k is dominated by the control parameter rather than by the size.

[15] C. Zener, Proc. R. Soc. London, Ser. A **137**, 696 (1932).

[16] N. V. Vitanov, Phys. Rev. A **59**, 988 (1999).